Comprehensive Analysis Identified and Validated CX3CR1 as Potential Biomarkers for Atherosclerosis

Hongxuan Li[1], Xin Liu[2,*], Yanhui Cen[1], Wei Jia[1], Bojia Li[1],

Xiaoying Qu[1], Qiyan Jin[1]

1. School of Basic Medicine, Guangxi University of Chinese Medicine, Nanning 530200, Guangxi, China

2. Faculty of Chinese Medicine Science, Guangxi University of Chinese Medicine, Nanning 530222, Guangxi, China

First author: 3385874884@qq.com(Hongxuan Li)

*Correspondence author: 694789947@qq.com(Xin Liu)

Abstract

Background: The etiology and disease development of atherosclerosis (AS) are still incompletely understood. In this research, we try to identify the gene biomarkers that play roles in the development and progression of AS and the relationship with immune cells.

Methods: By mining Gene Expression Omnibus (GEO) database, we acquired the dataset of AS for further research. After identifying the differentially expressed genes (DEGs) shared by AS and normal control samples, we performed functional enrichment analysis to them. Integrating the least absolute shrinkage and selection operator (LASSO) algorithm, support vector machine recursive feature elimination (SVM-RFE) algorithm, and random forest (RF) algorithm we ultimately selected genes candidates for the development of AS. Using CIBERSORT method, the difference of the immune infiltration of AS and normal control samples were analyzed. We also investigate the correlation of optimal gene biomarkers and specific several types of immune cells.

Results: DEGs were involved in the Toll-like receptor signaling pathways and Leukocyte transendothelial migration. Results of Gene Ontology (GO) analysis showed significant enrichment of DEGs in regulation of inflammatory response, leukocyte migration, and immune receptor activity. While Disease Ontology (DO) analysis indicated that DEGs are significantly enriched in terms including lung disease, atherosclerosis, coronary artery disease, and arteriosclerosis. CX3CR1 and C3 were screened by the LASSO, SVM-REF, and RF algorithms. AS samples showed relatively low infiltration levels of naive B cells (P<0.001), plasma cells (P<0.001), resting memory CD4 T cells (P<0.001), activated memory CD4 T cells (P<0.001), monocytes (P<0.001), M1 macrophages (P<0.001), M2 macrophages (P<0.001), activated dendritic cells (P=0.009), resting mast cells (P<0.001), and neutrophils (P=0.049) than normal controls, While AS samples harbored higher

infiltration levels of memory B cells (P<0.001), follicular helper T cells(P<0.001), gamma delta T cells (P<0.001), M0 macrophages (P<0.001), and activated mast cells (P<0.001) compared with normal control samples. We also identified non-negligible links between the expression levels of CX3CR1 and immune cells including M0 macrophages and M1 macrophages.

Conclusions: CX3CR1 played critical roles on the development of AS and had the potential as prognosis biomarkers for AS patients.

Keywords

Atherosclerosis, Biomarkers, GEO, Random Forest, SVM-REF, LASSO

1. Introduction

Atherosclerosis (AS) were known as a kind of a lipid-driven chronic inflammatory disease involving arterial wall. Factors including secondary inflammation, activation of vascular smooth muscle cells, recruitment of monocytes, accumulation of extracellular substances and lipids promote plaque formation. As the disease developing, plaque rupture and plaque erosion may lead to thrombosis and vascular occlusion, arising acute vascular events. AS are also accounted for the majority of cardiovascular diseases (CVD) and peripheral arterial disease (PAD) [1, 2]. Incidence rates for AS have risen sharply since 2017, the elevated mortality for AS of 31% also posed a serious threat to middle-aged and older adults[3]. The impact of chronic inflammatory response and immune-mediated Endothelial cell damage as well the precise molecular mechanisms promoting the development and progression of AS are only partially known AS are only partially known, calling for further systematic studies.

Except most general and widely accepted theory that the plaque formation was raised by the joint effects of Endothelial dysfunction in the area of arterial intimal blood flow disorder and subendothelial retention of lipoproteins and the vascular smooth muscle cell activation and the accumulation of extracellular and extracellular substances and lipids, Secondary inflammatory response and monocyte recruitment also play their roles in the pathogenesis of AS[4]. Prevention of atherosclerosis and associated atherosclerotic cardiovascular diseases is now rely on lifestyle changes such as exercise interventions and quitting smoking to reduce risk factors. Anti-platelet aggregation and hypolipidemic drugs were used to help delay the progress of atherosclerosis and prevent atherosclerotic plaque destabilization. Besides, interventional treatment is the main treatment option for treating coronary heart disease and other cardiovascular disease events. High morbidity and mortality associated with AS Calls for new treatment strategies to improve outcomes in this disease. The knowledge gaps of the underlying mechanisms of AS have hindered the development of effective therapeutic strategies[5]. Thus, there is urgent need to delineate the molecular pathogenesis of AS, identify potential therapeutic markers, and develop effective drugs.

It has become an international consensus defining AS as multifactorial disease caused and influenced by many pathways, such as abnormal lipid metabolic system, inflammatory reaction caused by monocyte infiltration, oxidative stress, dysfunction of vascular endothelial

cells and so on. Endothelial cell injury caused by oxidative stress due to the disorder of the anti-oxidant system in vivo implied the non-negligible role of oxidative stress in the occurrence and development of AS[6, 7]. Therefore, some researchers believe that restoring and strengthening the antioxidant capacity of the body to maintain the stability of the internal environment is the key for the treatment of AS.

Bioinformatics can efficiently and intuitively describe the molecular mechanism of disease at multiple levels and in multiple aspects, providing a large amount of effective information for basic medical research. The reactive oxygen species-related analysis and the establishment of biomarkers for AS-related biological information may provide an effective therapeutic potential for AS.

In this study, through bioinformatics analysis of AS datasets, the oxidative stress-related AS maker feature genes were screened out, and gene expression and ROC curve validation were performed in independent external datasets to provide an effective reference for the treatment of AS from the aspect of OS. Investigation of genes biomarkers as indicator revealing the immune status of AS is crucial to gain a deeper understanding of the molecular mechanisms involved in AS.

2. Materials and methods

2.1. Data Processing and Download of the AS Dataset

This study involved 69 AS cases and 35 control samples cases from Gene Expression Omnibus (GEO- https://www.ncbi.nlm.nih.gov/geo/) database with accession number GSE100927[8]. GSE57691 cohort based on GPL10558 which consisted of 9 AS samples and 10 control samples were obtained for the validation. Mining the GeneCards (https://www.genecards.org), we obtained 1399 oxidative stress (OS) related protein domains with relevance scores >7 for the subsequent identification of DEGs ， see Supplement table 1 in Appendix A).

Supplement File 1 ： shows the OS genes extracted from the GeneCards with a relevance score ≥ 7.

2.2. Identification of DEGs

Using “limma” R package, we identified the DEGs between AS and normal control samples with the filter criteria of fold change (FC) = 2 (|log2FC| >1; P <0.05). Those with log2FC >0 was considered upregulated genes and log2FC <0 downregulated genes. The “pheatmap” and “ggplot2” packages in R were respectively employed to visualize the heatmap and volcano plots for DEGs. Besides, a Venn diagram was plotted and displayed the number of OS-related hub genes obtained from the results of the two methods (DEGs and OS-related genes).

2.3. Functional enrichment analysis

GO and KEGG pathways analyses for the DEGs were performed to annotate the functions. The R package used for this operation includes “clusterProfile”, “enrichplot”, “ggplot2”, “org.Hs.eg.db”, “GOplot”, and “DOSE”. The significance of enriched processes was determined

using a cutoff of P value of 0.05. Adj P value <0.05 was used as the threshold to screen significantly enriched GO terms, DO terms, and KEGG pathways.

2.4. Screening of Feature Genes

Three machine-learning (ML) methods were used to screen feature genes. We applied three approaches to identify the feature genes. Using "glmnet" package in R, we performed LASSO regression to select the first part of feature genes. Optimal penalty parameter λ for LASSO regression was determined by minimal binomial deviance using 10-fold cross validation method. Using "e1071", "kernlab", and "caret" packages in R, we then applied another machine-learning approach, SVM-RFE algorithm to identify the second subset of feature genes. The SVM-RFE algorithm removes the feature with the lowest score (least ranked) in each iteration and train remaining features again for next iteration. The whole process iterates until this algorithm finally select feature genes. The selection of the third subset of feature genes were implemented with RF algorithm employing the "RandomForest" package in R. The intersection of the three subsets of feature genes obtained from the above three ML methods were taken and ultimately determined key feature genes.

2.5. Construction of receiver operating characteristic (ROC) curves

Receiver Operating Characteristic (ROC) curves were plotted by using "pROC" function in the R package to estimate the diagnostic performance[9].

2.6. Validation of the Feature Genes and ROC

Validation of diagnostic role of feature genes for AS were conducted in GSE57691 dataset.

2.7. Immune Infiltration Analysis by CIBERSORT

Heterogeneity of immune cell content between AS tissues and normal cartilage tissues were analyzed with CIBERSORT method to explore the immune cell infiltrations in various samples. The correlation of different immune cell types and feature genes were investigated using the "Corrplot" R package. Spearman rank correlation test was used for statistical significance tests.

2.8. Statistical analysis

The software R (R version 4.1.2; https://www.r-project.org/)was used for statistical tests and data visualization in this research. The significance of correlation was analyzed by the Spearman correlation test. P value were less than 0.05 indicating a significant difference. Indication of p-value summaries were as follow: *P < 0.05, **P <0.01, ***P < 0.001, and ****P < 0.0001.

3. Results

3.1. Identification of DEGs

A total of 1399 OS-related genes were identified. The entire analysis workflow of this study was presented in the Figure 1.

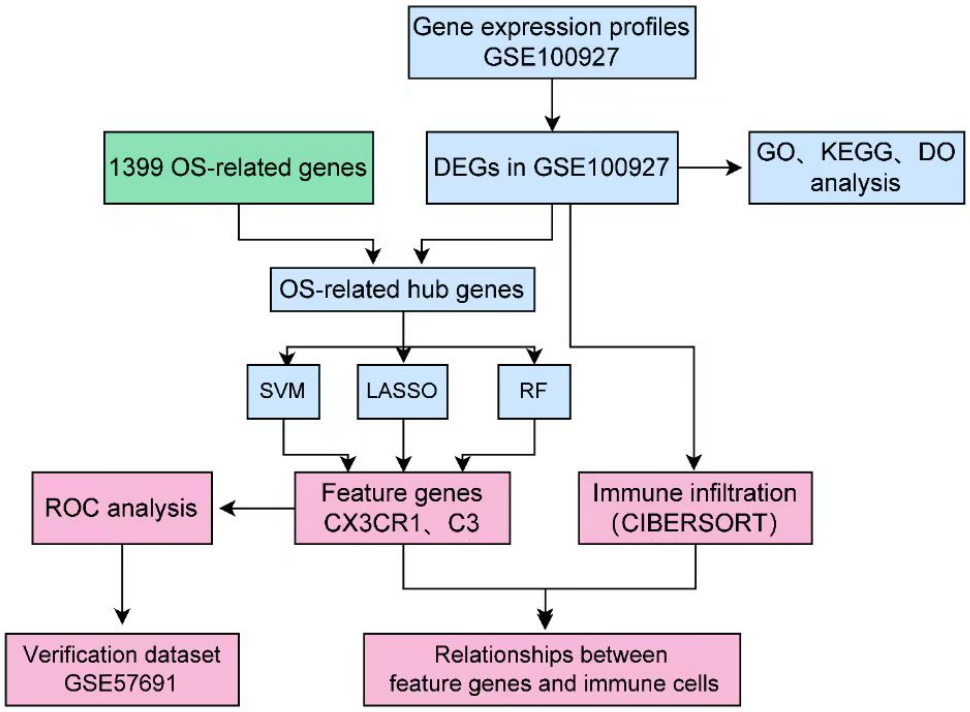

FIigure 1

In the difference analysis of the gene expression level between 69 AS samples and 35 normal controls samples from GSE100927, 295 up- and 123 down-regulated genes were screened. Identified DEGs were visualized by volcano plot and heat map in Figure 2A and 2B.

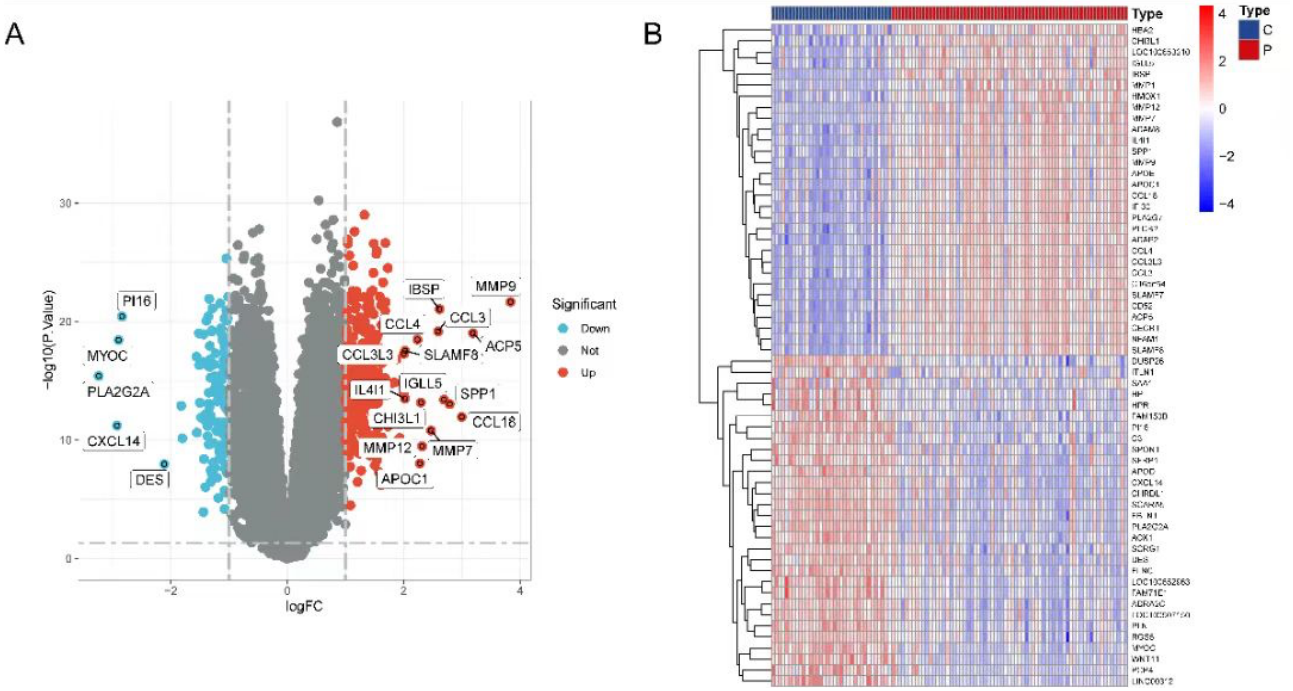

Figure 2A and 2B

3.2. Functional enrichment analysis

We ultimately identified 58 OS-related hub genes by intersecting the obtained DEGs and 1399 OS-related genes using the Venn diagram method ,see Figure 3A.

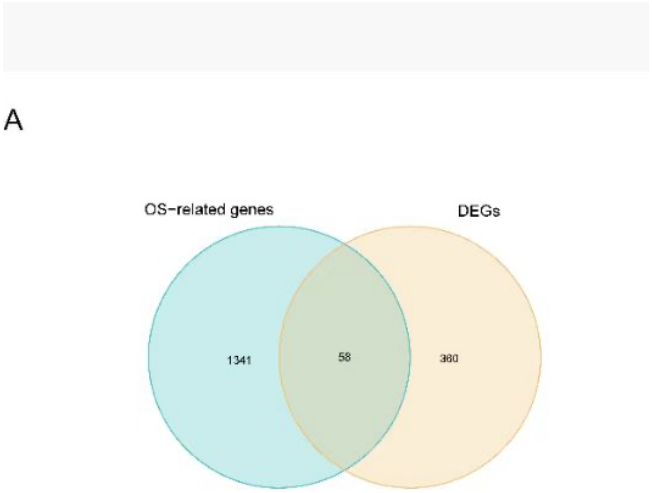

Figure 3A

Results of DO analysis showed significant enrichment of DEGs in various disease including lung disease, atherosclerosis, coronary artery disease, and arteriosclerosis,see Figure 3B.

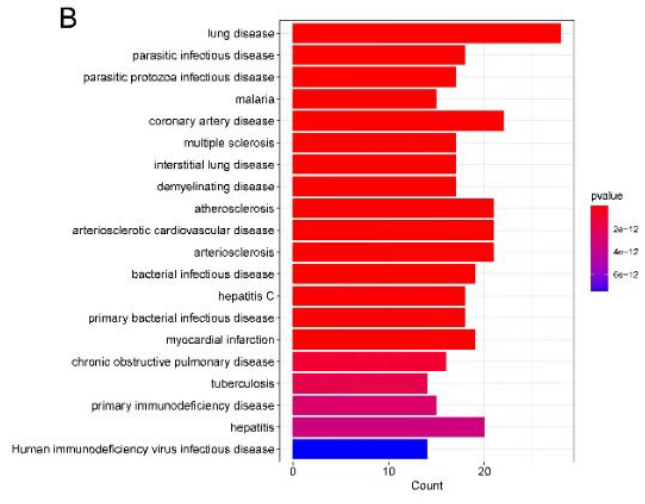

Figure 3B

The top-ten enriched GO terms in biological processes, cellular components and molecular functions from the GO enrichment analysis of the DEGs were represented in Figure 3C and DEGs were enriched in regulation of inflammatory response, leukocyte migration, and immune receptor activity. Results of KEGG pathway analysis on DEGs showed high abundance of Toll-like receptor signaling pathways and Leukocyte transendothelial migration ,see Figure 3D. Taken together, the DEGs were related with immune associated pathways.

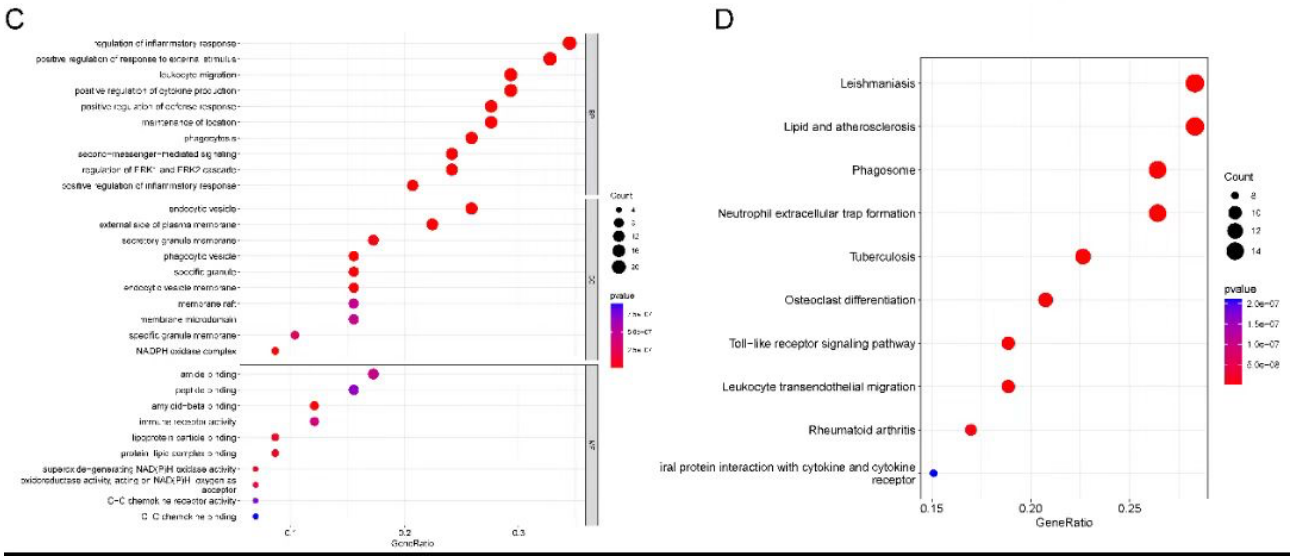

Figure3C and 3D

3.3. Selection of Feature Genes

Three machine algorithms simultaneously employed for the identification of feature genes, SVM-REF algorithm selected six genes from OS-related hub genes ,see Figure 4A, LASSO algorithm identified eight genes ,see Figure 4B and RF algorithm provided 20 key genes ,see Figure 4C.

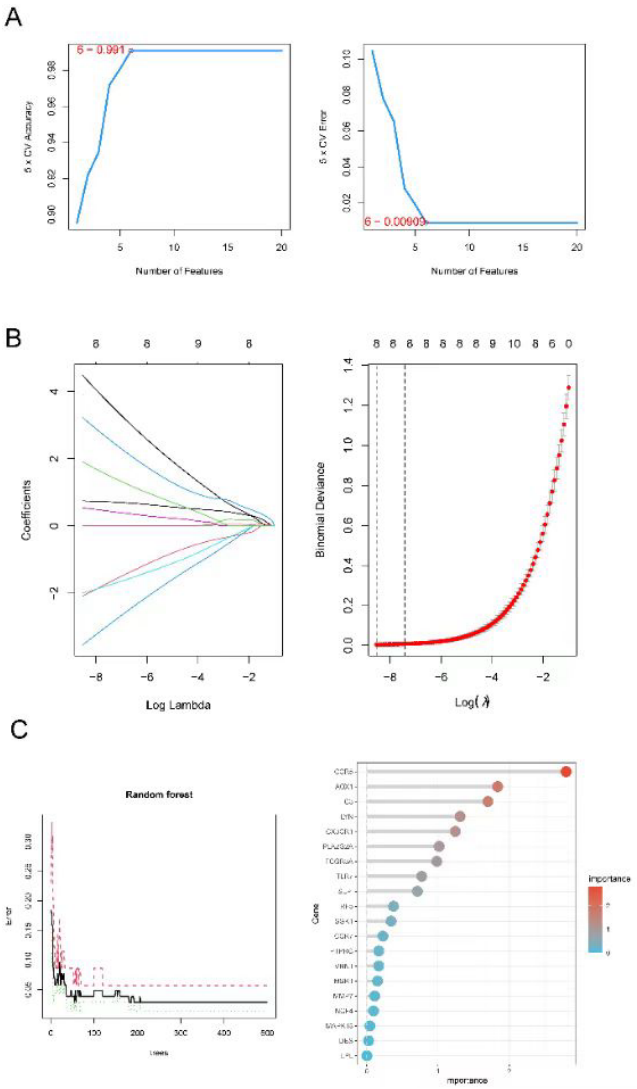

Figure 4A and 4B and 4C

Taking the intersection of the results of genes selection by the three ML methods, we ultimately obtained two feature genes: CX3CR1 and C3 ,see Figure 4D.

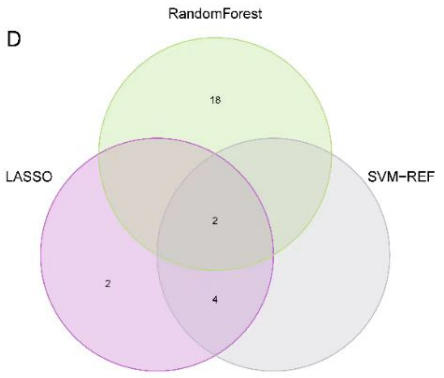

Figure 4D

Followed correlation analysis among the expression of the two genes all showed negative correlations ,see Figure 5.

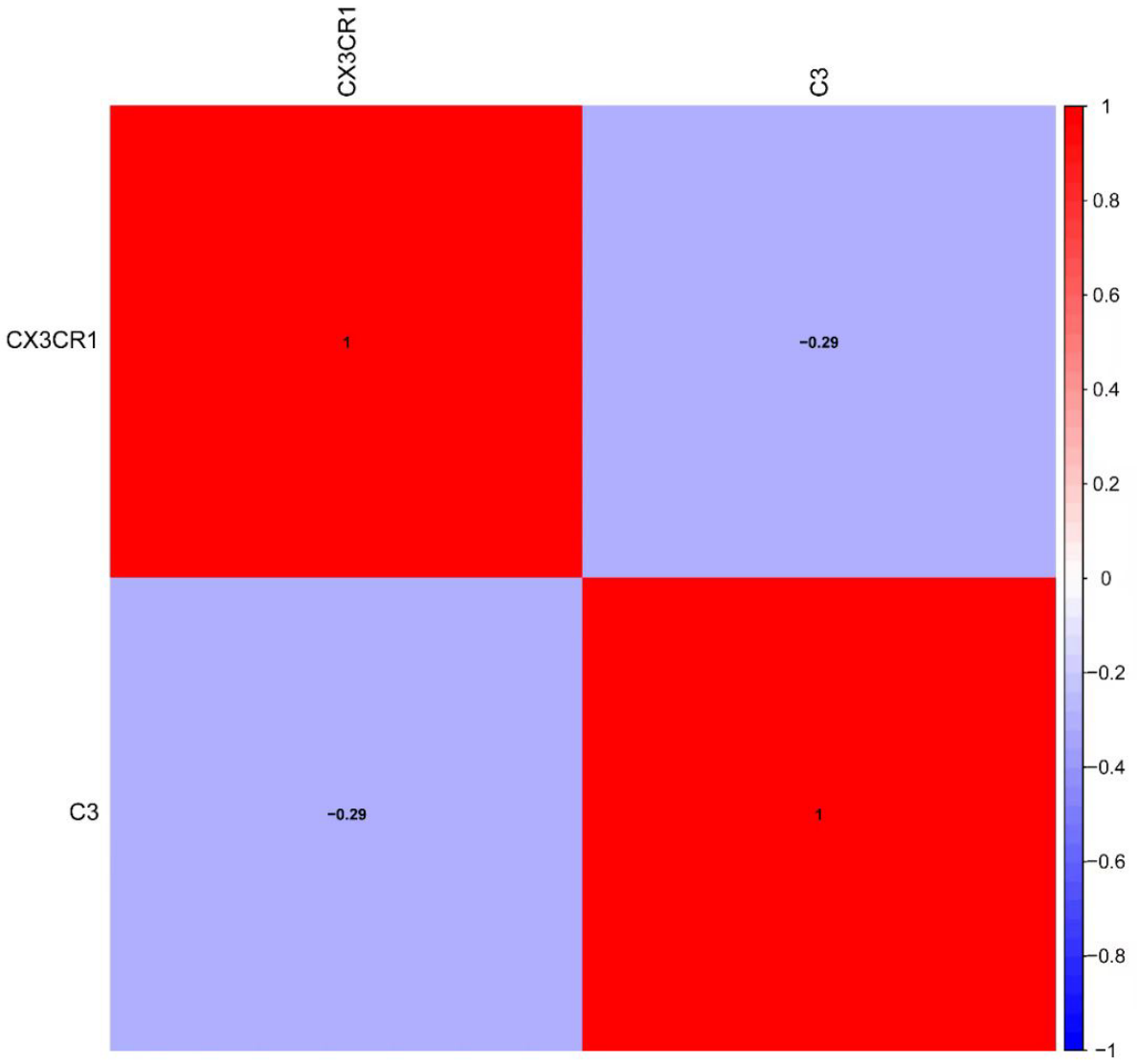

Figure 5

We then performed difference analysis in GSE100927 and reconfirmed that CX3CR1 mRNA expression was higher in AS than the normal samples, while the C3 mRNA expression was lower in AS than the normal samples， see Figure 6A and 6B.

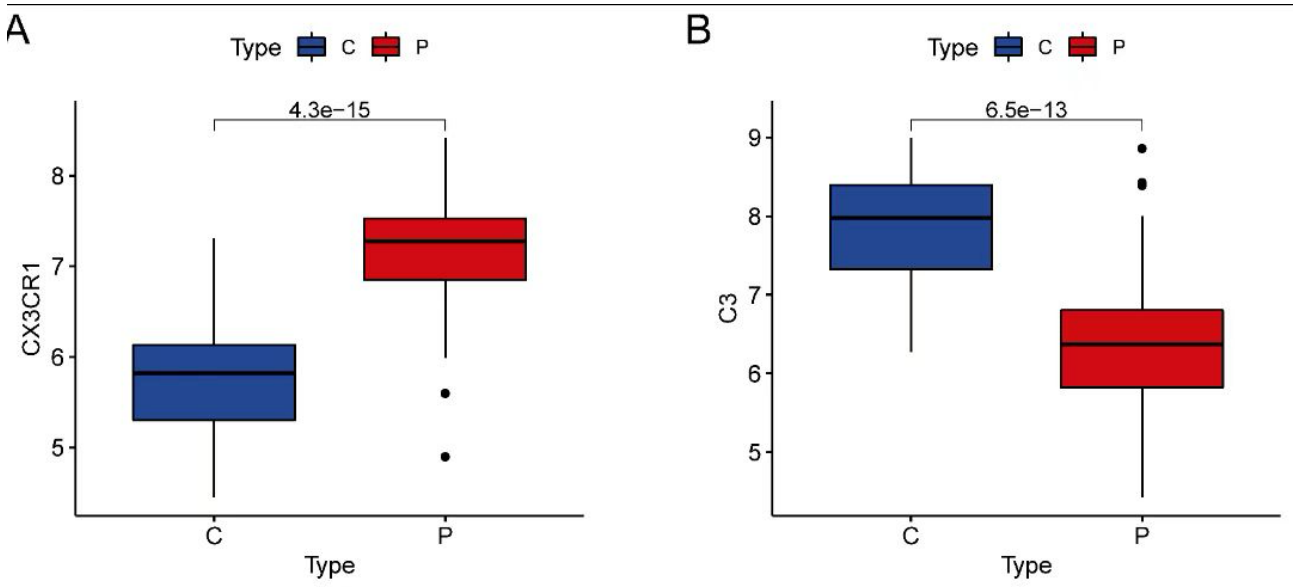

Figure 6A and 6B

The AUC of ROC analysis was 0.937 for CX3CR1, and 0.882 for C3 ， see Figure 6C and 6D.

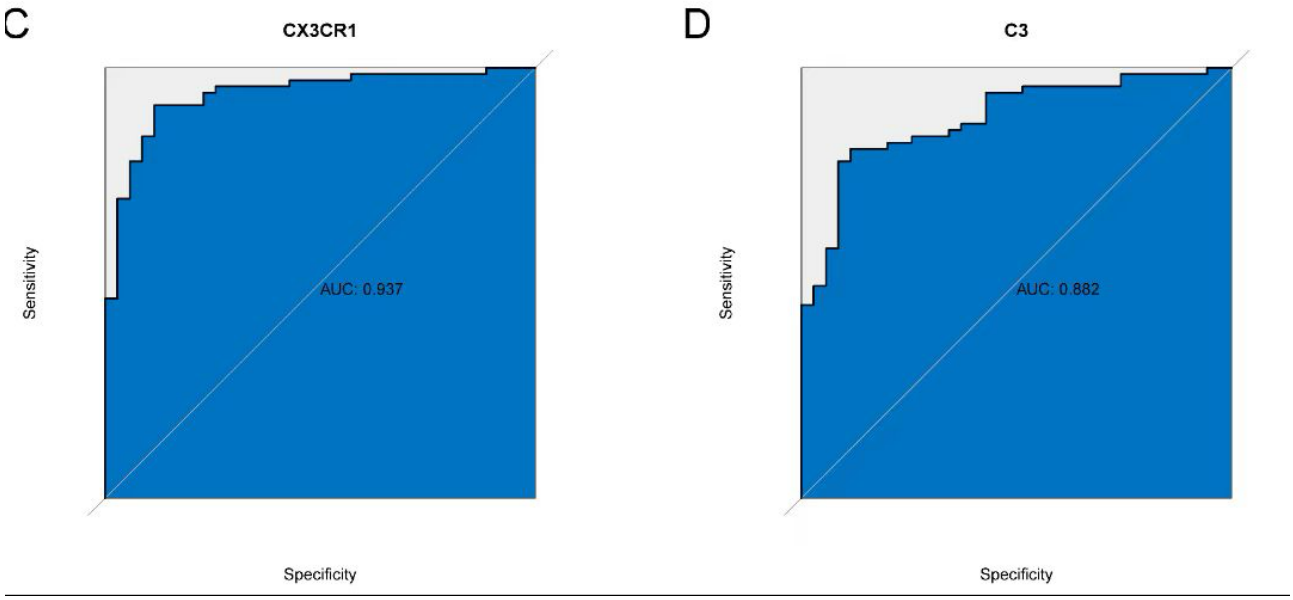

Figure 6C and 6D

3.4. Verification of the Feature Genes

The difference of the expression of the four hub genes between AS samples and corresponding normal tissue samples were confirmed again in the validation cohort GSE1919 dataset. The expression levels of CX3CR1 in AS samples tissue were higher compared with that in the normal tissue samples, while the C3 mRNA expression was no significance between AS and normal samples ,see Figure 7A and 7B.

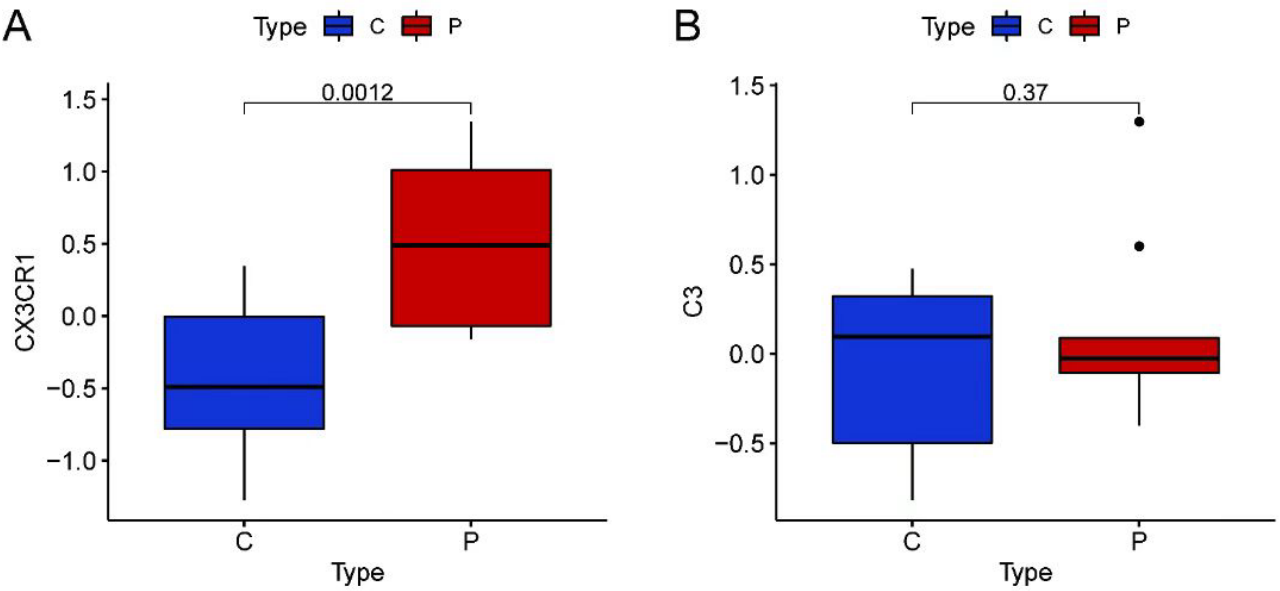

Figure 7A and 7B

The results of ROC analysis,see Figure 7C and 7D showed that AUC was 0.9 for CX3CR1, and 0.478 for C3, which led us to further focus on the important role of CX3CR1 in AS.

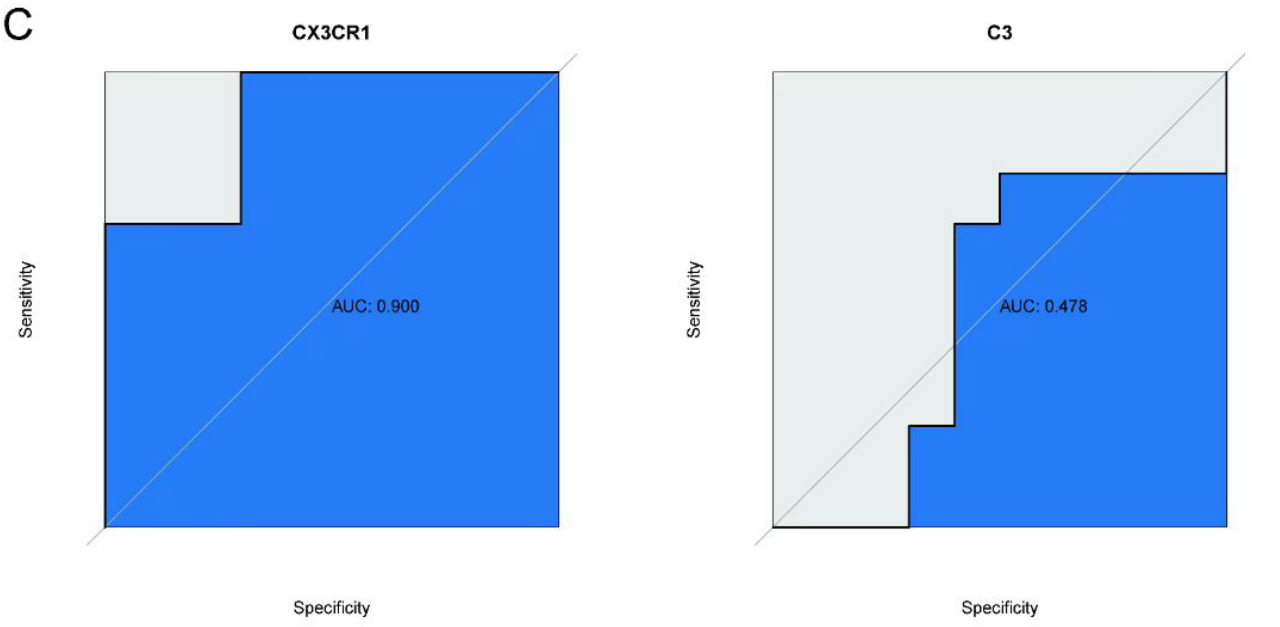

Figure 7C and 7D

3.5. Trait Gene Interaction Analysis

A PPI network of the feature genes was established using GeneMANIA database (Figure 8A) and result shown that CX3CL1 had a strong link to CX3CR1. GO and KEGG analysis of signature genes were subsequently performed.

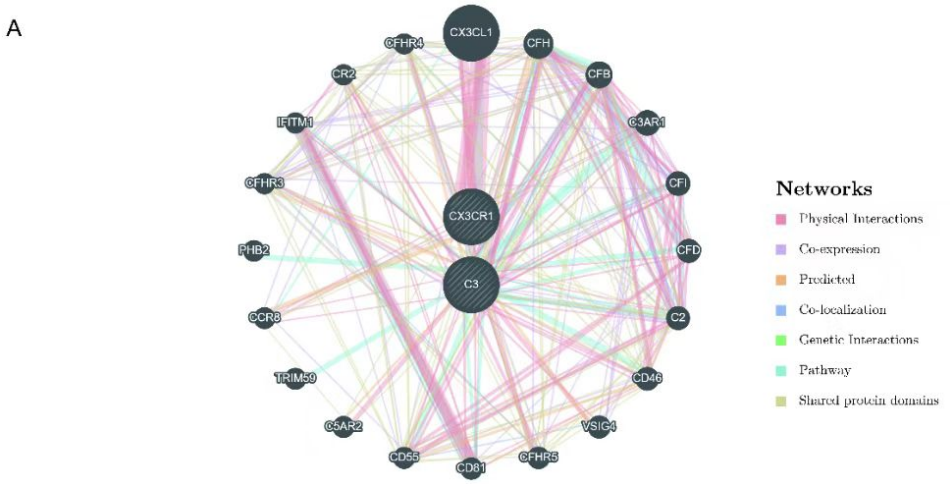

Figure 8A

Activation of immune response, humoral immune response, and regulation of immune effector process were the most abundant BP. In CC category, signature genes were mainly enriched in secretory granule membrane, primary lysosome, acrosomal membrane, and basal plasma membrane. In the MF part, immune receptor activity, complement binding, and chemokine receptor activity were significantly enriched ,see Figure 8B.

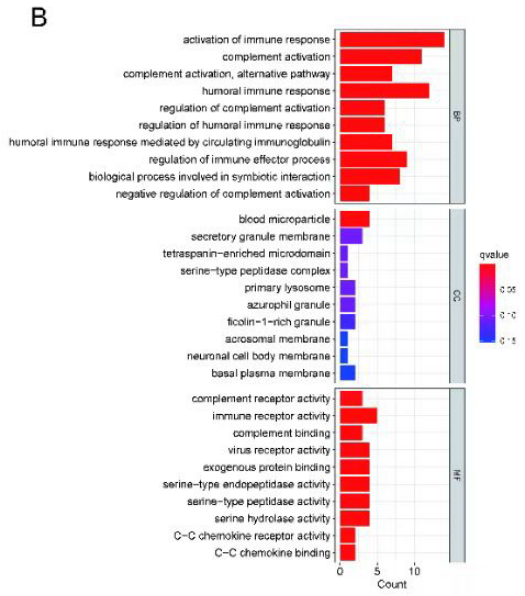

Figure 8B

The main enriched pathways, according to KEGG analysis, were B cell receptor signaling pathway, chemokine signaling pathway, and complement and coagulation cascades see Figure 8C

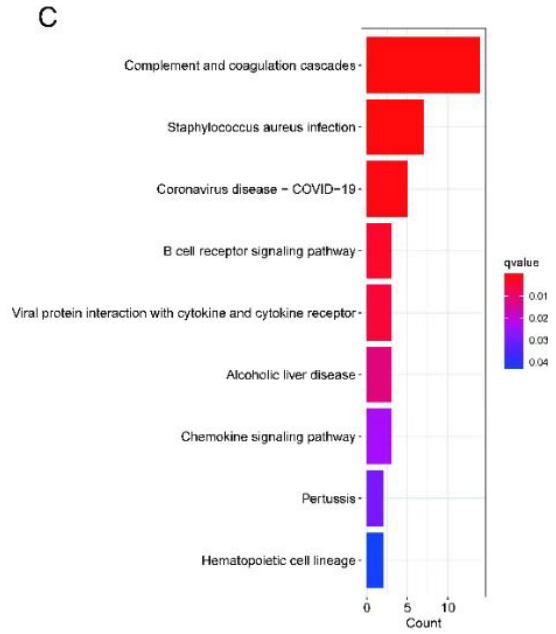

Figure 8C

3.6. Immunological Infiltration in the AS Group and Healthy Controls Using CIBERSORT Analysis

Above findings of the significantly abundant enrichment of DEGs in immune related function pathways prompted us to further explore the difference between AS and normal control samples in immune cell infiltration. The relative proportions of various kinds of immune cell in samples were plotted in Figure 9A.

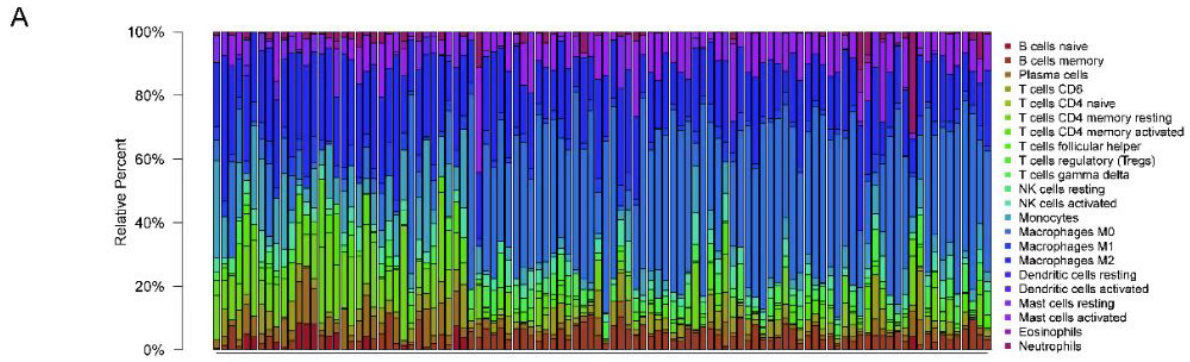

Figure 9A

the correlation among different immune cells were also analyzed ,see Figure 9B.

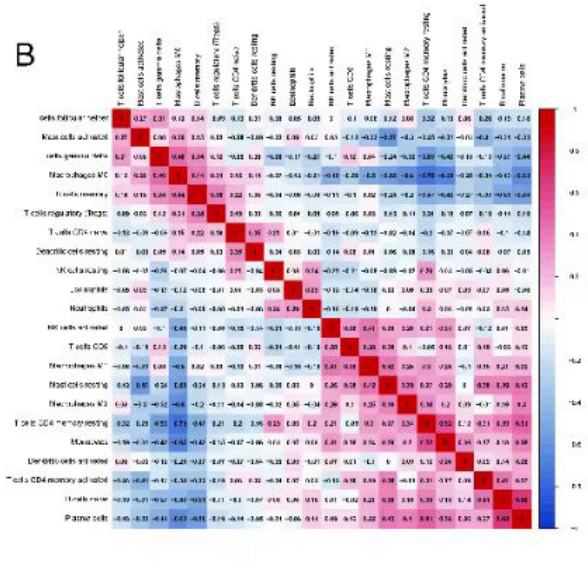

Figure 9B

Next, we investigated the correlation of the two gene signatures CX3CR1 and C3 and immune cell infiltration of AS to explore the potential of CX3CR1 and C3 as indicators of immune landscape for AS. AS patients had a lower proportion of naïve B cells (P<0.001), plasma cells (P<0.001), resting memory CD4 T cells (P<0.001), activated memory CD4 T cells (P<0.001), monocytes (P<0.001), M1 macrophages (P<0.001), M2 macrophages (P<0.001), activated dendritic cells (P=0.009), resting mast cells (P<0.001), and neutrophils (P=0.049) than normal controls, while the proportion of memory B cells (P<0.001), follicular helper T cells(P<0.001), gamma delta T cells (P<0.001), M0 macrophages (P<0.001), and activated mast cells (P<0.001) in AS patients were higher than normal controls ,see Figure 9C.

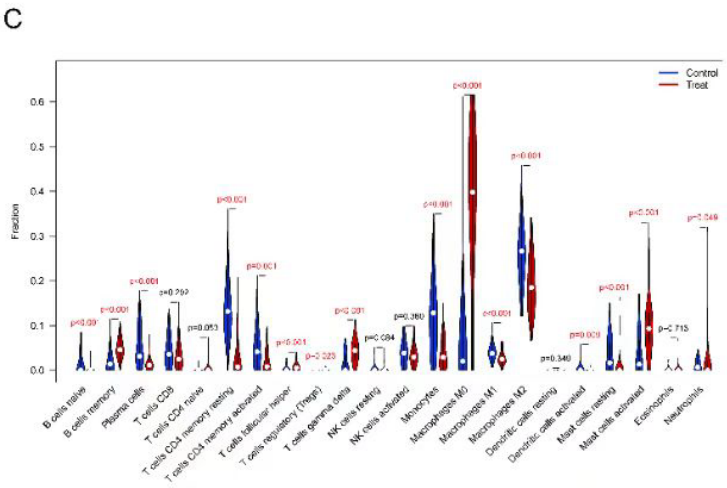

Figure 9C

The results of this analysis showed that there was a significant difference in the infiltration level between AS and normal controls. In addition, we found that the CX3CR1 was positively

correlated with memory B cells, Macrophages M0, Macrophages M1, gamma delta T cells and negatively correlated with naïve B cells, Monocytes, resting NK cells, Plasma cells ,see Figure 9D.

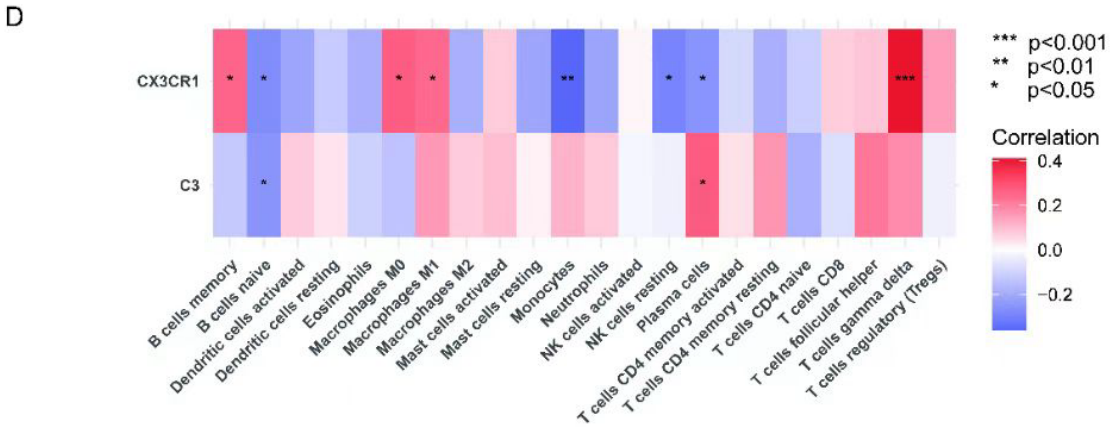

Figure 9D

4. Discussion

ROS levels and oxidative stress had been reported to be implicated in the pathogenesis of AS. One of the important links of AS were the impact of Ox-LDL oxidized by superoxide. Ox-LDL can induce the expression and release of inflammatory regulators, promote monocyte migration, increase the density of macrophage scavenger receptors, and increase the uptake of oxidized low density lipoprotein during foam cell formation, leading to the increasing risk of atherosclerotic lesions[10]. AS is a heterogeneous disease, and its pathogenesis is complex and poorly understood. Inflammatory responses and the modification of lipoproteins that cause lipid accumulation in AS are associated with imbalance of oxidative stress and immune processes[11]. However, few studies have focused on the aberrantly expressed gene biomarkers associated with immune infiltration and oxidative stress between AS and normal tissues.

The investigation to reveal the characterization of infiltrating immune cells in the AS would provide unique insights into the impact of Oxidative stress and its productions in the inflammatory infiltrate in AS and may lead to new therapeutic strategies to target ROS and immunobiology. Therefore, there is a compelling need to identify biomarkers that might be useful for diagnosing AS.

This study obtained 1399 OS-related genes from the GeneCards database. In this study, we screened 418 DEGs among which 295 were upregulated and 123 were downregulated. Result of followed functional analysis showed that DEGs significantly enriched at GO terms related to immune and inflammatory response, while results of KEGG enrichment analysis indicated that DEGs were closely related to Toll-like receptor signaling pathways and Leukocyte transendothelial migration. These findings suggested that DEGs play roles in inflammatory process in AS. We subsequentially performed Venn plot to selected the OS-related hub genes in AS with the intersection of 1399 OS-related genes and DEGs. By the combination of the three ML algorithms, we ultimately identified two feature genes CX3CR1 for further

exploration. Our result shown CX3CR1 expression was higher in AS than control cases. Followed ROC analysis of the two feature genes showed favourable discriminative and predictive abilities, suggesting the biological impact and potential diagnostic value of the two feature genes for AS. These results were validated in GSE57691 dataset.

It has been reported that CX3CL1 and CX3CR1 play important roles in vascular inflammation and injury and promote the formation of atherosclerosis[12]. An investigation on that correlation of chemokines and atherosclerosis focusing on the CX3CL1/CX3CR1 pathway reported that as a sort of soluble chemokine, CX3CL1 functions as a potent chemoattractant of monocyte recruitment in early atherosclerotic lesions, in more advanced stages of AS, it promotes anti-apoptosis and proliferation of vascular cells, affecting the synthesis and stability of atherosclerotic plaques[13]. CX3CR1 is the specific receptor of CX3CL1 and is mainly expressed in some leukocytes where it mediates migration, adhesion and proliferation[14], and coincidentally, CX3CL1-CX3CR1 axis activity were found to be elevated in patients with coronary artery disease (CAD)[15, 16], suggesting that CX3CL1/CX3CR1 axis might play a complex role in arteriosclerotic disease by influencing immune-related functions. There was also evidence indicated that CX3CR1 were derived from the differentiation of smooth muscle cells after vascular wall injury[17]. Besides, mouse models deficient in CX3CR1 display protection against atherosclerosis [18]. Previous research suggests that CX3CL1 and CX3CR1 play their parts in AS by promoting vascular wall inflammation[19, 20]. These findings suggest that CX3CR1 serve as a promising prognostic or diagnostic biomarker for AS and worth to be investigation in the future. Our previously study revealed that Seawater Pearl Hydrolysate (SPH) could inhibit oxidative stress status of vascular endothelial cells. According to our results, SPH might through impact the CX3CR1 mRNA expression, and then reverse the OS status of AS.

Many processes related to Macrophages including monocyte recruitment and differentiation, macrophage proliferation, death and egress, had been reported to be involved in the atherosclerotic plaque formation[21]. macrophage constituted the majority of cells components within the atheroma, some of them engorged with lipids resulting in dysregulated lipid metabolism due to noneffective regulation of the amount of cholesterol and ultimately become lipid-laden foam cells which were the characteristic pathologic cells of AS[22]. With the progress of the lesion, the phagocytic function of macrophages decreased, foam cell necrosis, cell membrane disintegration, lipid release, forming the lipid necrotic core of plaque[23]. In the late stage of AS, vascular endothelial cells die or apoptosis due to inflammation and activated killer T cells, coupled with matrix metalloproteinases (MMP) produced by peripheral macrophages induced by inflammation in local lesions and toxic substances released by necrotic cells, which decompose the collagen that makes up the fibrous cap, and the fibrous cap becomes thinner, coupled with the physical stress caused by the continuous expansion of the necrotic core. These factors eventually lead to AS plaque rupture, bleeding and thrombosis[24, 25]. The role of macrophages in the inflammation and immune response in AS were also explored in previous research. Using ESTIMATE algorithm, Shen et al. [26] calculated the immune scores and stromal scores of 29 atheromatous plaques samples and divided them into two groups, the ImmuneScoreH and ImmuneScoreL cluster for further analysis. They found higher level of M0 macrophages and higher enrichment of

immune-related pathways in atheromatous plaques samples in ImmuneScoreH cluster than that in ImmuneScoreL cluster, suggesting the difference in immune landscape of various atheromatous plaques. Their findings also indicated that atheromatous plaques with higher immune infiltration were more complex and be in more advanced stages.

It is worth mentioning that Shen et al. claimed that the immune landscape of plaques from the carotid arteries (most plaques belong to ImmuneScoreH cluster) differed largely from those plaques from the lower extremity arterials (most plaques belong to ImmuneScoreL cluster). Carotid atherosclerotic plaques tended to harbor more active immune response and higher infiltration levels of macrophages M0 in compared with plaques from other arteries[26, 27]. Similar results were also observed in our research. Compared with that in normal control samples, higher infiltration level of M0 macrophages and lower infiltration level of M1 macrophages of atheromatous plaques samples from GSE100927 (most plaques from the carotid arteries) were observed. In the correlation analysis on AS samples, we observed significantly positive correlation among oxidative stress-related CX3CR1 and macrophages M0 and macrophages M1. Our findings and speculations in this study, however, need to be validated and extended by experimental proof and further investigation.

5. Conclusion

This research identified the correlation among gene signatures CX3CR1 and the immune infiltration in AS, suggesting the potential of CX3CR1 as the indicator of the immune landscape and prognostic signature for AS. Besides, targeting CX3CR1 and related pathways represent new and innovative therapeutic strategies.

Acknowledgements

We thank the GEO datasets for providing data support to this study.

Authors' contriibutions

This research was conducted in collaboration with all authors. Xin Liu and Bojia Li designed and analyzed the research study. Hongxuan Li, Yanhui Cen, Wei Jia, Jiang Lin, Rui Yang, Zeping Huang, Zhiying Ning, Sen Li and Wei Huang wrote and revised the manuscript. Hongxuan Li collected and analyzed the data, and all authors have read and approved the manuscript.

Funding

This study was supported by grants from the National Natural Science Foundation of China (NSFC) (Grant no. 82260861), Guangxi University of Traditional Chinese Medicine's "Guipai Xinglin Top notch Talents Project"(Grant no. 2022C002), Guangxi University of Traditional Chinese Medicine Guipai Traditional Chinese Medicine Inheritance and Innovation Team Funding Project(Grant no. 2022B004), Middle-Aged and Young Teachers' Basic Ability

Promotion Proj ect of Guangxi (Grant no. 2021KY0291), 2022 Guangxi University of Traditional Chinese Medicine key postgraduate scientific research innovation project (Grant no. YCSZ2022003), Open Project for the Construction of First Class Disciplines in Guangxi(Grant no. 2019XK137), Innovation and Entrepreneurship Training Program for College Students at Guangxi University of Traditional Chinese Medicine(Grant no.202210600017，202010600018),University level research project of Guangxi University of Traditional Chinese Medicine(Grant no. 2019MS001), Key Project of Guangxi First Class Discipline Construction Project(Grant no. 2018XK023,2018XK024).

Availability of data and materials

The data underlying this article will be shared on reasonable request to the corresponding author.

Ethics approval and consent to participate

Ethnical is not applicable because these data are from public database.

Consent for publicationO

Not applicable.

Competing interests

The authors declare that they have no conflict of interest.

Figure legend

Figure 1 : Flowchart of the study.

Figure 2 : Differential expression analysis. (A) Volcano plot showing the differential expressed genes. significantly upregulated genes (red), significantly downregulated genes (green), non-differentially expressed genes (Brown). (B) The heatmap displaying the expression levels difference of DEGs between AS samples and normal controls samples.

Figure 3 : The identification of key module genes and relevant function enrichment analysis. (A) Venn diagram showing the intersection shared by DEGs and OS-related genes. (B) DO terms. (C) GO analysis. (D) KEGG analysis.

Figure 4 : Feature genes selecting process by the three algorithmics. (A) Gene selection using the SVM–RFE algorithm. (B) Gene selection using the minimum absolute shrinkage and selection operator model (lasso). (C) Random Forest error rate versus the number of classification trees. The top 20 relatively important genes were selected. (D) The Venn diagram showing the intersection or union of genes selected by the three algorithmics.

Figure 5 : Correlation between trait genes.

Figure 6 : Gene expression of the feature genes and ROC curves. (A) The different expression levels of CX3CR1 and C3 between AS and normal controls samples in the GSE100927 (B) The ROC for the evaluation of predictive power of CX3CR1 and C3 to predict the prognosis for AS.

Figure 7: Validation of the feature genes and ROC curves. (A) Expression of CX3CR1 and C3 in AS patients compared to normal controls in the validation dataset (GSE57691 dataset). (B) ROC curves of the predictive efficacy of CX3CR1 and C3 in the validation set.

Figure 8 : Interaction analysis of feature genes. (A) Characterized gene co–expression network. (B) GO analysis of co–expressed genes. (C) Co–expressed gene KEGG analysis.

Figure 9 : Immune cell infiltration analysis. (A) The relative proportions of different immune cell subtypes in AS samples. (B) Correlation matrix showing the correlation among different kind of immune cells. (Red) positive correlation. (Blue) Negative correlation. Darker colors indicate higher P value of correlation. (C) Violin plots showing the difference of infiltration of various immune cell subtypes between AS and normal control samples. (D) The correlation between feature genes and immunity cells. *p < 0.05, **p < 0.01, ***p < 0.001.

References

[1] Kong, Q., et al., Increased serum visfatin as a risk factor for atherosclerosis in patients with ischaemic cerebrovascular disease. Singapore Med J, 2014. 55(7): p. 383-7.

[2] Tern, P.J.W., et al., Site and Burden of Lower Limb Atherosclerosis Predicts Long-term Mortality in a Cohort of Patients With Peripheral Arterial Disease. Eur J Vasc Endovasc Surg, 2018. 56(6): p. 849-856.

[3] Stefanadis, C., et al., Coronary Atherosclerotic Vulnerable Plaque: Current Perspectives. J Am Heart Assoc, 2017. 6(3).

[4] Niccoli, G., et al., Role of Allergic Inflammatory Cells in Coronary Artery Disease. Circulation, 2018. 138(16): p. 1736-1748.

[5] Kelly, P.J., et al., Anti-inflammatory approaches to ischaemic stroke prevention. J Neurol Neurosurg Psychiatry, 2018. 89(2): p. 211-218.

[6] Irace, F.G., et al., Role of Oxidative Stress and Autophagy in Thoracic Aortic Aneurysms. JACC Basic Transl Sci, 2021. 6(9-10): p. 719-730.

[7] Perrotta, I. and S. Aquila, The role of oxidative stress and autophagy in atherosclerosis. Oxid Med Cell Longev, 2015. 2015: p. 130315.

[8] Barrett, T., et al., NCBI GEO: archive for functional genomics data sets--update. Nucleic Acids Res, 2013. 41(Database issue): p. D991-5.

[9] Robin, X., et al., pROC: an open-source package for R and S+ to analyze and compare ROC curves. BMC Bioinformatics, 2011. 12: p. 77.

[10] Liao, Y., E. Zhu, and W. Zhou, Ox-LDL Aggravates the Oxidative Stress and Inflammatory Responses of THP-1 Macrophages by Reducing the Inhibition Effect of miR-491-5p on MMP-9. Front Cardiovasc Med, 2021. 8: p. 697236.

[11] Wójcik, P., et al., Oxidative Stress and Lipid Mediators Modulate Immune Cell Functions in Autoimmune Diseases. Int J Mol Sci, 2021. 22(2).

[12] McDermott, D.H., et al., Chemokine receptor mutant CX3CR1-M280 has impaired adhesive function and correlates with protection from cardiovascular disease in humans. J Clin Invest, 2003. 111(8): p. 1241-50.

[13] Apostolakis, S. and D. Spandidos, Chemokines and atherosclerosis: focus on the CX3CL1/CX3CR1 pathway. Acta Pharmacol Sin, 2013. 34(10): p. 1251-6.

[14] Liu, P., et al., CX3CR1 deficiency impairs dendritic cell accumulation in arterial intima and reduces atherosclerotic burden. Arterioscler Thromb Vasc Biol, 2008. 28(2): p. 243-50.

[15] Xueyao, Y., et al., Circulating fractalkine levels predict the development of the metabolic syndrome. Int J Endocrinol, 2014. 2014: p. 715148.

[16] Zhang, H., et al., Hydrogen sulfide inhibits the development of atherosclerosis with suppressing CX3CR1 and CX3CL1 expression. PLoS One, 2012. 7(7): p. e41147.

[17] Rowinska, Z., et al., Role of the CX3C chemokine receptor CX3CR1 in the pathogenesis of atherosclerosis after aortic transplantation. PLoS One, 2017. 12(2): p. e0170644.

[18] mai, T., et al., Identification and molecular characterization of fractalkine receptor CX3CR1, which mediates both leukocyte migration and adhesion. Cell, 1997. 91(4): p. 521-30.

[19] Imai, T. and N. Yasuda, Therapeutic intervention of inflammatory/immune diseases by inhibition of the fractalkine (CX3CL1)-CX3CR1 pathway. Inflamm Regen, 2016. 36: p. 9.

[20] Apostolakis, S., et al., CX3CR1 receptor is up-regulated in monocytes of coronary artery diseased patients: impact of pre-inflammatory stimuli and renin-angiotensin system modulators. Thromb Res, 2007. 121(3): p. 387-95.

[21] Moore, K.J., et al., Macrophage Trafficking, Inflammatory Resolution, and Genomics in Atherosclerosis: JACC Macrophage in CVD Series (Part 2). J Am Coll Cardiol, 2018. 72(18): p. 2181-2197.

[22] Brophy, M.L., et al., Myeloid-Specific Deletion of Epsins 1 and 2 Reduces Atherosclerosis by Preventing LRP-1 Downregulation. Circ Res, 2019. 124(4): p. e6-e19.

[23] Shapouri-Moghaddam, A., et al., Macrophage plasticity, polarization, and function in health and disease. J Cell Physiol, 2018. 233(9): p. 6425-6440.

[24] Moore, K.J., F.J. Sheedy, and E.A. Fisher, Macrophages in atherosclerosis: a dynamic balance. Nat Rev Immunol, 2013. 13(10): p. 709-21.

[25] Moore, K.J. and I. Tabas, Macrophages in the pathogenesis of atherosclerosis. Cell, 2011. 145(3): p. 341-55.

[26] Shen, Y., et al., Identification of potential therapeutic targets for atherosclerosis by analysing the gene signature related to different immune cells and immune regulators in atheromatous plaques. BMC Med Genomics, 2021. 14(1): p. 145.

[27] Martinet, W., et al., Macrophage Death as a Pharmacological Target in Atherosclerosis. Front Pharmacol, 2019. 10: p. 306.

Appendix A

Supplement table 1:

shows the OS genes extracted from the GeneCards with a relevance score ≥ 7.

Gene Symbol	Relevance score	Gene Symbol	Relevance score	Gene Symbol	Relevance score	Gene Symbol	Relevance score	Gene Symbol	Relevance score
KIT	7	DECR1	8.25	GFM2	9.92	HTR2C	12.35	APOA1	16.69
NDUFA13	7.01	NR1H2	8.26	SETX	9.92	ENO1	12.36	CYGB	16.76
MAPK13	7.01	HBEGF	8.27	ADAMTS13	9.93	LAMP2	12.37	CCND1	16.8
TNFSF4	7.02	AKAP9	8.28	GHRL	9.94	ITGB1	12.37	PDHA1	16.81
LEPQTL1	7.02	MIR34C	8.3	KCNMA1	9.94	SERPINA1	12.37	ASS1	16.88
MIR185	7.03	MSR1	8.3	MIR125A	9.95	S100B	12.37	LRRK2	16.9
ALS3	7.04	RPA1	8.31	H2AX	9.96	LOC110973015	12.37	HTR2A	16.92
ALS7	7.04	RCAN1	8.32	FOXP3	9.96	REST	12.4	DRD2	16.94
OXTR	7.05	FTH1	8.32	KRT8	9.97	PIK3R1	12.4	SLC6A3	16.96
DHFR	7.05	CYP11A1	8.32	PLA2G2A	9.98	CDC42	12.4	MAPKAPK2	17.07
ACACA	7.05	CHGA	8.33	BRF2	9.98	CXCL12	12.4	ARG1	17.08
GPX8	7.05	PLCB1	8.33	MIR200B	9.98	DAO	12.41	GGT1	17.1
BGLAP	7.06	SENP3	8.33	FKRP	9.98	BAK1	12.41	SLC25A4	17.11
TAZ	7.07	RRM2B	8.33	ADPRS	9.99	HCRT	12.41	NPY	17.12
MAPK12	7.08	PDK1	8.34	H4-16	9.99	ADORA2A	12.43	GBA	17.2
YBX1	7.08	SNCB	8.34	ALAD	9.99	MTHFR	12.46	BMP6	17.24
SFXN4	7.09	MIR107	8.34	MIR181A1	10	CSF3	12.47	HSPD1	17.28
SLC4A1	7.09	MIR181C	8.36	MT-ND4	10.01	BRCA1	12.47	CYP1B1	17.3
HPSE	7.09	CAPN3	8.36	NDUFB9	10.01	GNAS	12.48	NOX1	17.34
RPTOR	7.09	RNASE3	8.36	IGF2	10.02	SIGMAR1	12.48	HP	17.35
MTA1	7.1	PRPH	8.37	ACTN2	10.04	IREB2	12.5	LEP	17.37
CD274	7.1	CFI	8.37	ISCU	10.04	TGFBR1	12.5	BLVRB	17.4
ENDOG	7.1	LAMP1	8.39	XIAP	10.05	CARS2	12.51	NOS1AP	17.42
BMP4	7.1	BLOC1S1	8.39	CFLAR	10.05	CALM3	12.52	FARS2	17.5
MTTP	7.11	PML	8.39	GSTA2	10.06	MAP2	12.56	HRAS	17.53
TCF7L2	7.11	CCK	8.39	NLRP3	10.07	MIF	12.56	CALCA	17.54
TLR6	7.11	TIMP2	8.4	QDPR	10.08	CTSD	12.56	RAC1	17.59
VDR	7.12	TRAF2	8.41	CASP2	10.1	MAPKAPK3	12.58	SNAP25	17.61
CPQ	7.12	STIP1	8.42	SRF	10.12	PAH	12.59	PRKAA2	17.63
NFU1	7.12	NOSTRIN	8.42	PKLR	10.13	OXR1	12.6	PRKAA1	17.66
GADD45G	7.12	MYLK	8.43	TYMP	10.14	CACNB4	12.61	EPO	17.66
FMO4	7.13	GSTM5	8.43	SCO1	10.14	PXN	12.61	MSRB2	17.68
BBC3	7.14	TPK1	8.43	PTS	10.14	HTR3A	12.62	LOX	17.68

AREG	7.14	SLC2A4	8.43	THBS1	10.19	IGF2R	12.62	NDUFB8	17.72
HK1	7.15	HLA-A	8.44	SYP	10.2	CASP7	12.65	PDE5A	17.73
PIK3R2	7.15	UNG	8.44	TYK2	10.2	GSTO2	12.66	CRYAB	17.74
ATG5	7.16	IL3	8.46	GRN	10.21	ANG	12.66	EGFR	17.83
POU5F1	7.16	RORA	8.46	OPTN	10.22	EPHA3	12.66	RPS27A	17.83
SIRT6	7.16	MDH1	8.46	GRIA1	10.22	PTPN22	12.67	MDM2	17.85
MIR214	7.17	RUNX2	8.46	PIK3CB	10.22	MRPS16	12.67	THBD	17.87
JAZF1	7.18	SCARA3	8.46	IKBKB	10.23	GLUD2	12.74	NDUFV1	17.87
FADD	7.18	PDIA3	8.47	CEBPB	10.23	CREBBP	12.75	CTLA4	17.89
BCL2A1	7.2	DDC	8.47	CD80	10.23	SLC25A13	12.75	MIR22	17.96
IL11	7.2	GSTM4	8.47	C4B	10.23	SIRT3	12.75	MAPK9	17.98
SELENOT	7.2	PIGA	8.48	PPP1R15A	10.23	GSTA4	12.77	NGF	18
MAP3K11	7.2	BRCA2	8.48	ACSL4	10.24	IDH2	12.79	IL2	18.07
CYP4F2	7.21	UNC13A	8.49	EIF2B3	10.24	TOR1A	12.84	SRC	18.08
MIR24-2	7.21	VPS13C	8.49	PLA2G4A	10.25	DCTN1	12.84	CREB1	18.08
ASPA	7.22	TNFSF11	8.49	TUBA1B	10.26	MIR17	12.86	ATF6	18.21
ROCK1	7.24	CYP2C8	8.5	STK11	10.27	C12orf65	12.86	MIR146A	18.25
NEDD8	7.26	SERPINF1	8.5	MMP3	10.27	EPHX1	12.88	TLR2	18.3
GAA	7.27	DYSF	8.51	GRM5	10.29	TGFBR2	12.88	ATM	18.34
ATP5PD	7.27	PSIP1	8.51	DRD3	10.29	BCHE	12.91	SDHD	18.43
PEPD	7.28	TPI1	8.52	SMARCA4	10.3	ERCC6	12.93	IL1A	18.48
CAPN2	7.29	PDGFRB	8.52	NTRK1	10.31	NFE2L1	12.93	NDUFS3	18.56
PTPRC	7.3	CAMK2G	8.52	ECE1	10.31	EIF2AK2	12.94	MT-ATP6	18.57
CYP20A1	7.3	EPHX2	8.53	LYN	10.32	ADM	12.95	MT-CYB	18.6
MKI67	7.31	CR1	8.53	ELK1	10.32	H2AC18	12.96	CDKN1A	18.61
SORL1	7.31	CYP3A5	8.54	ALDH3A1	10.35	COL2A1	12.98	OSGIN1	18.63
MIR210	7.31	AGRN	8.54	PDCD1	10.37	TRPV1	12.99	SLC1A3	18.66
SORD	7.33	NR2C2	8.57	CCS	10.38	VIP	13	ATF4	18.67
MUC5AC	7.33	XRCC6	8.58	SIL1	10.39	SYK	13	GTPBP3	18.69
ALDH3A2	7.33	PPP3CA	8.59	IL5	10.4	A2M	13.01	RHOA	18.71
CHCHD2	7.33	UBQLN1	8.59	PSEN2	10.41	ALOX5	13.01	PPARA	18.75
PLD1	7.34	FOXO4	8.6	ARG2	10.41	CD44	13.02	ABL1	18.77
C5	7.34	MAPK7	8.6	IDO1	10.42	IAPP	13.02	KDR	18.82
MIR222	7.35	NES	8.6	DYNLL1	10.44	PRKCA	13.03	SPP1	18.82
TNFRSF11B	7.36	FTL	8.6	MTR	10.45	SNCAIP	13.04	ACAD9	18.93
TNFRSF10A	7.37	BACH1	8.61	PDIA2	10.45	S100A8	13.04	AGT	18.99
FABP1	7.37	SCGB1A1	8.61	SLPI	10.46	NAGS	13.04	TRPM2	18.99
PFKM	7.37	FMO2	8.61	SLC1A1	10.46	HNRNPA1	13.04	GSTT1	19.01
PYCR2	7.38	APC	8.63	EIF2B4	10.46	ATP13A2	13.05	PIK3CA	19.12
IL6R	7.38	MYD88	8.63	ADAM17	10.48	SLC25A3	13.07	PRDX1	19.19
SUMO1	7.39	HERPUD1	8.64	CAMP	10.48	DAPK1	13.08	HMGB1	19.19

TEK	7.4	CYP17A1	8.64	CYP2A6	10.48	TTR	13.09	CLU	19.2
SLC7A1	7.4	TYRP1	8.65	HDAC1	10.48	EIF4E	13.11	PIK3CG	19.26
FIG4	7.4	XRCC5	8.65	CD79A	10.52	DLST	13.14	CDKN3	19.29
GLT8D1	7.4	FKBP1B	8.66	CYP27A1	10.52	CRYAA	13.14	HBB	19.45
LBR	7.41	MMP14	8.66	RXRA	10.54	UBE2L3	13.16	NDUFA12	19.49
CXCL16	7.41	TMEM161A	8.67	PTPN1	10.55	NEFH	13.16	SELP	19.5
OSM	7.42	ALOX15	8.68	EP300	10.57	G3BP1	13.17	ATP5F1A	19.57
GRIN1	7.42	SOX2	8.68	CXCR3	10.57	ADH1C	13.21	SERPINE1	19.6
DYRK1A	7.42	ASL	8.68	NAT2	10.59	DNMT1	13.21	C1QBP	19.63
MIR181A2	7.42	CCNF	8.68	EDNRA	10.59	MRPS22	13.23	PRDX3	19.65
DNM2	7.43	DIABLO	8.69	PFN1	10.59	TFAM	13.24	TXNRD1	19.72
TACO1	7.43	MMP7	8.69	MT-ND3	10.6	OSGIN2	13.24	SLC22A5	19.73
GIGYF2	7.43	TRPV4	8.7	NTHL1	10.6	CCL3	13.25	MSRB1	19.74
C5AR1	7.44	PGK1	8.7	KCNJ2	10.61	SCN4A	13.26	AGER	19.79
ALDH3B1	7.44	NDUFA1	8.7	NRG1	10.62	UCHL1	13.26	PRL	19.82
CCR7	7.44	IL23A	8.7	CHCHD10	10.63	MIR195	13.27	LDLR	19.85
MUC1	7.45	ATXN1	8.71	BECN1	10.64	FGFR1	13.29	CTNNB1	19.87
CANX	7.45	JUNB	8.71	CLEC4A	10.66	OXT	13.3	TRDN	19.88
ADH1A	7.45	HSPA14	8.71	COQ2	10.66	MIR34A	13.32	CASQ2	19.93
FRZB	7.46	CD86	8.72	EIF4EBP1	10.67	AKR1A1	13.34	PC	19.94
EEF2	7.47	GAL	8.72	SGK1	10.7	OPA1	13.34	CALM1	19.94
ZFAND1	7.47	FGF7	8.73	ANGPT1	10.7	VARS2	13.34	ETFB	20.01
UBQLN4	7.47	SCP2	8.73	SOCS3	10.71	SLC1A2	13.35	SHC1	20.05
PKD1	7.47	BCL6	8.73	UCP1	10.71	CRHR1	13.36	COMT	20.07
MIR200C	7.47	SULT1A3	8.74	MIR93	10.72	POR	13.37	ANXA5	20.11
TNIP1	7.48	GADD45A	8.74	AIF1	10.73	PRKG1	13.37	MMP2	20.24
SCN4B	7.49	GSN	8.75	IL15	10.73	TGFB3	13.37	TH	20.37
IL16	7.5	MDH2	8.75	TRIM21	10.75	KCNJ5	13.37	SELE	20.42
H3C14	7.5	IL2RB	8.76	LTA	10.76	BACE1	13.39	STAT3	20.45
ARNT	7.5	ABCC8	8.76	NAMPT	10.77	SNTA1	13.39	NUDT1	20.47
CYP19A1	7.51	PPIG	8.77	MIR29A	10.77	DRD5	13.41	MT-CO1	20.54
SDC1	7.51	MCU	8.77	MFN2	10.77	SERPINA3	13.41	MIR21	20.55
CACNA2D1	7.52	MLYCD	8.78	CALM2	10.77	HSPA9	13.41	EIF2S1	20.64
AQP1	7.52	CHMP2B	8.78	TIA1	10.78	SCN2A	13.42	EIF2AK3	20.7
CDC25C	7.52	UBC	8.79	RELA	10.79	AMPD1	13.44	TNFRSF1A	20.73
ACTN4	7.53	MSN	8.79	NGFR	10.79	TNFRSF1B	13.47	TERT	20.74
BSG	7.55	PTPN3	8.79	TRAP1	10.8	ITPR1	13.47	IL13	20.85
LYRM4	7.55	NTF4	8.8	HGF	10.81	TSFM	13.47	GDNF	20.89
KL	7.56	SLC19A3	8.8	GAP43	10.82	MT-TK	13.49	SLC2A1	20.92
ANXA11	7.56	CCNB1	8.8	MIR433	10.83	MIR223	13.49	FAS	20.96
AVP	7.56	FMR1	8.8	SLC6A2	10.83	TGFB2	13.52	SOD3	21.02

ABCC3	7.56	HSPA6	8.81	CD4	10.83	UCP3	13.54	MB	21.09
MRAP	7.56	HK2	8.82	MYO9A	10.84	IDH1	13.55	MT-ND1	21.17
FANCD2	7.57	SELL	8.83	PENK	10.86	CSF1	13.55	SDHA	21.2
FIS1	7.57	PRKCZ	8.83	EPRS1	10.86	DNM1L	13.55	CYP1A2	21.25
PGAM5	7.57	PTGIS	8.85	CDH1	10.87	MET	13.57	SDHB	21.29
CAMKK2	7.57	ZC3H12A	8.85	CFTR	10.88	TSC2	13.63	NR3C1	21.3
CFAP410	7.58	AHR	8.87	RPS6KA5	10.89	PLA2G6	13.66	MMP9	21.3
VIPR1	7.58	GLS	8.87	PVALB	10.89	PGD	13.69	TXN2	21.32
ADRB3	7.59	PPOX	8.87	MRPL44	10.89	KCNH2	13.69	OXSR1	21.36
RTN4	7.59	NCAM1	8.88	CTSB	10.91	HMOX2	13.69	HSPA8	21.4
MIR19A	7.6	RETN	8.88	NTS	10.91	PPIF	13.71	C9orf72	21.45
FAAH	7.6	B2M	8.89	ERBB4	10.92	EHHADH	13.73	GFAP	21.51
GLA	7.61	CD55	8.89	EIF4G1	10.93	TXNRD2	13.77	IGF1	21.52
PDE4A	7.61	VKORC1L1	8.89	KLF4	10.93	AKR1B1	13.78	TPO	21.58
TARS2	7.61	SLC25A27	8.89	CYP2B6	10.93	GSTM2	13.79	EGF	21.61
CX3CR1	7.62	EDNRB	8.9	ACE2	10.94	MAP2K3	13.79	MYH7	21.72
NOD2	7.62	PF4	8.91	SESN1	10.94	NGB	13.8	MSRA	21.75
SFTPB	7.62	SMAD2	8.91	NRF1	10.95	MMP1	13.81	CYP2E1	21.76
LANCL1	7.63	SOCS1	8.91	PECAM1	10.95	NCF1	13.81	GCH1	21.77
CD38	7.63	BLK	8.94	KLF2	10.96	MECP2	13.81	ELAC2	21.87
FECH	7.64	PYGM	8.94	GSS	10.96	NPPB	13.87	MAOB	21.96
TPPP3	7.65	CDK6	8.95	EIF2AK1	10.96	SIRT2	13.9	PRDX6	22.03
IL1RAPL2	7.65	MICB	8.95	FLT1	10.96	STAT1	13.92	CYP1A1	22.34
TP53INP1	7.65	PPARD	8.96	RPS6KB1	10.96	ECHS1	13.93	PINK1	22.38
ENC1	7.65	UBQLN2	8.99	OXA1L	10.98	AOC3	13.93	GPX3	22.42
PEX5	7.66	HYOU1	9	ATXN3	10.99	H6PD	13.94	ACADL	22.44
IKBKG	7.66	TACR1	9.01	HLA-B	11.01	FGF2	13.94	SP1	22.49
FYN	7.66	BDKRB2	9.01	ATF3	11.01	GPX2	13.94	NOX4	22.67
ABCG2	7.66	ADRB1	9.02	RAF1	11.03	GLRX2	13.95	CASP9	22.79
MIR199A1	7.67	CTTN	9.03	MALAT1	11.04	OSER1	13.95	F2	22.83
UCN2	7.67	DEPDC5	9.03	ADA	11.04	GSTM3	13.97	ETFA	22.88
CD46	7.68	MIR106B	9.04	MAPK11	11.04	KRIT1	13.97	PPARG	22.88
KIAA0319L	7.68	NQO2	9.04	GRIN2B	11.04	SDHAF1	13.99	HTRA2	22.97
MIR184	7.68	ABCC2	9.04	ANXA2	11.06	OPRM1	14.01	ADIPOQ	23
CXCL2	7.68	SREBF1	9.05	COX6B1	11.08	SESN2	14.05	CYP3A4	23.06
GPX5	7.69	SERPINH1	9.05	HMGCL	11.08	APOH	14.05	ALDH2	23.14
CD28	7.7	H2BC21	9.06	CXCR4	11.08	VDAC1	14.06	FOXO3	23.38
YAP1	7.7	LPA	9.07	CXCL10	11.09	REN	14.07	COX5A	23.46
GADD45B	7.7	VCL	9.07	MMP13	11.09	SST	14.08	SELENON	23.56
EIF2AK4	7.71	MIR145	9.08	MIR122	11.12	ADRB2	14.09	OGG1	23.62
NEK1	7.71	MIR143	9.09	STK39	11.12	NR3C2	14.11	KNG1	23.67

HDAC9	7.71	FASN	9.1	GCLM	11.14	GSK3B	14.11	MTOR	23.71
ACAD8	7.71	CASP4	9.1	TLR3	11.15	KRAS	14.15	CHAT	23.77
MIR203A	7.72	CD34	9.11	BAD	11.15	MYC	14.15	ABCD1	23.89
ADAM10	7.72	KRT18	9.11	TBP	11.17	ADH5	14.15	MTO1	24.03
MT-CO3	7.72	CTSG	9.12	CCN2	11.18	HTR1A	14.15	TLR4	24.05
RAG2	7.73	SLC11A2	9.12	TJP1	11.18	FXN	14.16	BAX	24.15
C3	7.74	ODC1	9.12	ALDH9A1	11.2	NPPA	14.16	PRDX2	24.22
HRH2	7.75	TNFRSF10B	9.13	BIRC5	11.2	PTK2	14.19	POLG	24.4
VEGFC	7.76	CHEK1	9.13	FCGR3B	11.21	CPT1B	14.19	MAPK3	24.43
SLC8A1	7.76	SFTPD	9.13	PDGFRL	11.21	HLA-DRA	14.26	VCAM1	24.45
MRPS34	7.76	CD69	9.14	NLRP1	11.22	UGT1A1	14.28	HSF1	24.45
FCGR3A	7.77	PDLIM4	9.14	KCNE1	11.23	PRKD1	14.3	NCF2	24.62
IL12B	7.78	GH1	9.14	GAD1	11.23	CYB5R3	14.33	PRNP	24.79
CIITA	7.78	LPL	9.14	ENO2	11.24	GPX4	14.34	FOS	24.94
SIAH1	7.79	HNF1A	9.14	PEX12	11.25	GPT	14.35	MAOA	25.05
MIR23B	7.79	SCARB1	9.15	CDKN1B	11.26	FMO3	14.39	APOE	25.05
SET	7.79	PTX3	9.15	GJA1	11.27	F3	14.39	HIF1A	25.17
MIR92A1	7.81	RAD51	9.16	HSPA1B	11.27	TFRC	14.41	CACNA1C	25.18
MMD	7.81	EZH2	9.16	LOC111365141	11.28	JAK2	14.41	CASP8	25.25
ITGA2	7.81	COX15	9.16	FGF1	11.3	MT-TL1	14.41	LMNA	25.28
TLR5	7.81	LGALS1	9.17	DRD4	11.31	IL1R1	14.41	XBP1	25.28
PHYH	7.82	GRIN2A	9.19	IRF1	11.31	MAP2K1	14.45	CRH	25.53
HSPG2	7.82	VAPB	9.2	ATF2	11.31	MT-CO2	14.48	PPARGC1A	25.65
PRDM10	7.82	ELAVL1	9.2	CDK1	11.33	ATP2A2	14.52	CAV1	26.16
RBP4	7.83	HRH1	9.22	RNF112	11.33	PLA2G7	14.52	PON2	26.18
DYNC1H1	7.84	ATR	9.23	HMGCR	11.34	CD40	14.53	BCL2	26.23
HPRT1	7.85	PNKP	9.24	DHCR24	11.34	MAP2K4	14.56	TARDBP	26.28
SPARC	7.85	GFER	9.24	NTRK2	11.34	GSTO1	14.56	MAPK10	26.31
SELENOK	7.85	CDH5	9.25	CXCL1	11.35	TPH1	14.57	HSPA1A	26.33
MAPK8IP1	7.86	MIR24-1	9.25	AHSP	11.35	BCL2L1	14.58	ACE	26.46
TFEB	7.87	ABCA1	9.25	NDUFA6	11.36	ACHE	14.64	APEX1	26.49
TAT	7.88	DAXX	9.25	PLCG1	11.37	CRAT	14.66	OLR1	26.49
HDAC2	7.88	CDH2	9.26	IRAK1	11.37	GCLC	14.68	ESR1	26.5
VNN1	7.88	GZMB	9.27	FMO1	11.38	NFKBIA	14.68	MAP3K5	26.53
MIR142	7.88	CALB2	9.28	HSP90AB1	11.39	SGCB	14.71	VCP	26.6
GDF15	7.89	MUTYH	9.29	ITGAL	11.39	IL4	14.75	AIFM1	26.64
SORCS2	7.89	ERCC8	9.29	AKT2	11.4	UCP2	14.77	ICAM1	26.7
MIR152	7.89	DDAH1	9.3	FDXR	11.41	NR4A2	14.83	CP	26.94
SELENOP	7.89	NDUFS7	9.3	MIR126	11.41	CD40LG	14.86	SCN5A	26.98
ADSL	7.9	NDUFS6	9.31	CCR6	11.42	IL17A	14.88	HSPB1	27.11

NEFL	7.9	ERO1A	9.32	KIF1B	11.43	EGR1	14.89	BDNF	27.3
HPX	7.91	DSP	9.32	DSPP	11.45	LOC110806262	14.9	NFKB1	27.4
OTC	7.92	NDUFA10	9.34	CCNA2	11.46	TRMT10C	14.92	PRDX5	27.52
LCAT	7.92	SUMO2	9.34	CPOX	11.46	PNPT1	14.92	HBG2	27.57
RYR3	7.92	NRAS	9.36	ALDH1A1	11.46	CDKN2A	14.94	CAV3	27.57
ISG15	7.93	IGF2BP1	9.36	HSPB2	11.47	PTK2B	14.96	TYR	27.6
MAP3K1	7.93	CXCL9	9.36	CNTF	11.47	CCL5	15.01	KEAP1	27.7
BCR	7.93	SLC18A2	9.39	MT3	11.48	NPM1	15.05	GSTM1	27.84
SLC25A1	7.94	PIK3C2A	9.39	SDHAF2	11.5	ETS1	15.05	AARS2	27.95
EPHA4	7.94	BCL2L11	9.4	EPAS1	11.5	PRODH	15.1	FOXO1	27.96
MAPKAPK5	7.95	STK4	9.41	LONP1	11.51	ACO1	15.13	PSEN1	27.99
ACTG1	7.95	HNF4A	9.42	ABCC1	11.51	EEF1A1	15.17	DDIT3	28.04
CLIC1	7.97	ALOX12	9.42	SETD2	11.53	OGDH	15.18	GSTP1	28.09
SLC7A11	7.98	GLS2	9.43	E2F1	11.55	TAC1	15.23	CPT1A	28.1
TLR8	7.98	CFH	9.46	MTFMT	11.59	CASP1	15.27	SLC25A20	28.34
NCF4	7.98	F8	9.47	CALB1	11.6	CYP11B2	15.27	GPX1	28.43
DGKQ	7.99	DNAJB1	9.48	MBP	11.61	NDUFAF2	15.28	SQSTM1	28.47
IFNAR1	8	TBK1	9.48	S100A9	11.62	PRKCD	15.29	ETFDH	28.53
MMP8	8	ITIH4	9.49	NDUFS1	11.63	SLC5A7	15.29	HSPA5	28.54
CDKN2B	8	LRPPRC	9.49	IGF1R	11.66	SMAD3	15.31	ACOX1	28.56
TOP1	8	XRCC1	9.5	CHUK	11.67	ENG	15.32	CYP2D6	28.87
ACO2	8.01	TP73	9.5	DNASE1	11.67	GLUL	15.33	VWF	28.87
MIR25	8.02	ANGPT2	9.5	IFNB1	11.7	HSD17B4	15.34	NDUFS4	28.94
CUL3	8.03	AOX1	9.51	VIM	11.7	RAC2	15.4	GAPDH	29.13
DUOX1	8.03	NEAT1	9.51	ANK2	11.72	MT-ND2	15.42	MAPT	29.16
CAMK4	8.04	NME1	9.52	MAP2K7	11.73	PON3	15.42	PARP1	29.43
CUL1	8.04	DES	9.53	CR2	11.74	ATXN2	15.44	VEGFA	29.48
CYB5A	8.04	TRPA1	9.54	DLG4	11.75	PTEN	15.46	RYR2	29.56
IGF2BP2	8.04	TGFA	9.55	DRD1	11.76	TSPO	15.47	CCL2	29.85
UBE2D2	8.04	MAP3K7	9.55	PCNA	11.77	ELANE	15.48	HADHB	29.98
FAM120A	8.05	EPX	9.56	ADCY10	11.78	SDHC	15.49	RYR1	30.4
AQP4	8.05	PLG	9.56	PLAT	11.79	TUFM	15.55	CYBB	30.6
PDGFB	8.05	INSR	9.56	TSC1	11.8	ERN1	15.57	GFM1	30.79
MIR27A	8.05	RHOD	9.57	ELN	11.81	POMC	15.59	HSPA4	31.1
KCNE2	8.06	GP1BA	9.57	MBL2	11.82	DBH	15.61	PTGS2	31.12
HAMP	8.07	LGALS3	9.58	BMP2	11.83	CYP2C9	15.63	SNCA	31.58
BACH2	8.08	CYC1	9.58	LCN2	11.85	GPX7	15.63	IFNG	31.62
PPP5C	8.09	BAG3	9.58	GLUD1	11.86	P4HB	15.64	NQO1	31.87
AURKA	8.1	PARK12	9.59	TNFSF10	11.88	FUS	15.69	HSP90AA1	31.95
TLR7	8.1	STAT4	9.6	DMD	11.89	MT-ND5	15.7	EDN1	32.13
PTPA	8.11	NR1H4	9.6	MCL1	11.89	FASLG	15.7	TGFB1	32.32

WRN	8.11	DNAH8	9.6	NOL3	11.9	HLA-DRB1	15.74	JUN	32.45
TTPA	8.12	MT-ND6	9.6	CST3	11.91	MIR155	15.75	CYBA	32.63
RARA	8.12	NDUFA9	9.61	CBS	11.92	TF	15.8	CXCL8	32.79
UCN	8.12	FCGR2B	9.61	NDUFS8	11.92	CHKB	15.81	CRP	33.11
PKP2	8.13	CSK	9.62	CHKA	11.96	CDK2	15.87	ALB	33.45
KCNT1	8.13	STK24	9.63	DDAH2	11.99	CD36	15.9	SIRT1	33.85
ATXN8OS	8.13	AR	9.63	NTF3	11.99	HFE	15.91	ACADS	33.91
PARK10	8.13	GYG1	9.64	ACTB	12	ACP1	15.95	HADH	34.03
PARK16	8.13	PRKD2	9.69	PRKAB1	12	GSTA1	15.97	AKT1	34.11
PARK21	8.13	PPIA	9.69	STUB1	12.02	NOTCH1	16.03	INS	34.82
MGMT	8.14	CDK4	9.71	FCGR2A	12.02	DUSP1	16.05	IL10	35.03
LIN28B	8.15	TPT1	9.71	ITGB2	12.04	PRDX4	16.08	ACADVL	35.49
SMPD1	8.15	COA8	9.72	MATR3	12.05	PTPN11	16.08	TXN	35.54
GRM1	8.15	IRF5	9.72	APOB	12.06	AGTR1	16.12	CASP3	35.93
DMPK	8.15	F5	9.72	STK25	12.06	HSP90B1	16.13	G6PD	36.15
PYCR1	8.16	SCO2	9.72	TLR9	12.06	SLC18A3	16.13	MAPK1	36.3
UTRN	8.16	PKM	9.74	CSF2	12.07	FN1	16.15	SLC6A4	36.52
MIR148B	8.17	GLO1	9.74	APAF1	12.08	PRKCB	16.18	ACADM	37.37
FOXJ1	8.18	MYH6	9.74	PDYN	12.08	CNR1	16.19	IL1B	37.44
MIR144	8.19	MME	9.75	OPRD1	12.09	TREM2	16.22	CYCS	38.24
CCR5	8.2	FOXM1	9.75	TNFAIP3	12.09	NDUFV2	16.23	MAPK8	38.51
SLC40A1	8.2	ACOX2	9.76	ABCB1	12.09	GLRX	16.24	HADHA	38.55
ITGB3	8.2	JAK1	9.78	TGM2	12.1	ITGAM	16.27	PRKN	38.63
CCL11	8.21	H19	9.78	ACTA1	12.12	TECRL	16.27	IL6	38.95
MECOM	8.21	NDRG1	9.78	MIR23A	12.14	IL1RN	16.28	PON1	40.21
MIR20A	8.21	PEX11B	9.79	GRB2	12.17	CACNA1S	16.28	PARK7	40.56
DUSP19	8.22	ERBB2	9.79	HSD17B10	12.21	HTT	16.31	GSR	42.22
VASP	8.22	FKBP5	9.82	MRPS14	12.23	PLAU	16.33	XDH	43.46
HAO1	8.22	MIR133B	9.82	MIR132	12.24	TIMP1	16.35	APP	43.81
MIR9-1	8.22	TPM1	9.82	LTF	12.26	CDK5	16.36	MAPK14	44.95
FH	8.22	MIR221	9.82	CCL4	12.26	CALR	16.41	MPO	45.08
CYP21A2	8.23	VHL	9.83	NDUFS2	12.26	MGST1	16.45	SOD2	48.82
CACNA1A	8.23	IL2RA	9.84	BTD	12.26	SUOX	16.46	CPT2	49.36
BRAF	8.23	MSH2	9.84	IFNA1	12.26	PTGS1	16.5	NFE2L2	54.46
NOSIP	8.23	C4A	9.86	RB1	12.27	CYP2C19	16.58	TP53	57.5
KLRK1	8.23	RAB5A	9.86	SMAD4	12.27	TREX1	16.61	NOS1	58.58
ESR2	8.24	PLAUR	9.86	MAP2K6	12.31	TTN	16.61	HMOX1	60.47
PIK3C3	8.24	NEIL1	9.87	SRXN1	12.31	DLD	16.63	TNF	63.9
VTN	8.24	SPR	9.88	LPO	12.31	ADCYAP1	16.67	CAT	70.77
IL33	8.25	LCK	9.88	HBA1	12.32	CS	16.67	NOS2	71.08
CXCR1	8.25	MSRB3	9.89	IRS1	12.32	TXNIP	16.67	SOD1	80.41
PRKCG	8.25	GLE1	9.89	SLC17A5	12.34	IL18	16.67	NOS3	82.97

TALDO1	8.25	TAF15	9.91	KCNQ1	12.34	GCDH	16.67